[(^{t}Bu$_2$PCH$_2$SiMe$_2$)$_2$N]RuMe$_2$: Synthesis and Reactivity of an Unsaturated Ruthenium Dialkyl Radical Species

Michael J. Ingleson, Maren Pink, John C. Huffman, Hongjun Fan, and Kenneth G. Caulton*

Department of Chemistry & Molecular Structure Center, Indiana University, Bloomington, Indiana 47405

Received October 4, 2005

The reaction of PNPRuCl (PNP = (^{t}Bu$_2$PCH$_2$SiMe$_2$)$_2$N$^-$) with excess MeLi at −78 °C, followed by addition of a one-electron oxidant, leads to the thermally stable (at 25 °C), low-spin, five-coordinate trivalent ruthenium complex PNPRuMe$_2$, **1**. For comparison PNPRuI$_2$, **2**, was also synthesized and shown equally to be a low-spin d^5 complex. Compound **1** reacts with NO to produce the diamagnetic ruthenium(II) complex PNPRuMe$_2$(NO), **3**, with H$_2$ to give PNPRu(H)$_3$, **5**, and with excess CO to produce PNPRu(COMe)CO, **6**. The unusual stability of **1** is suggested to arise from the steric encapsulation of the radical center provided by the extremely bulky pincer ligand, the low coordination number (5), and a non-redox-innocent amide functionality.

Introduction

The organometallic chemistry of monometallic, trivalent Ru complexes is significantly underdeveloped, especially when compared to the plethora of work involving Ru^{II}.[1] This is in part due to the inherent presence of at least one "metal-based" unpaired electron, rendering NMR spectroscopy less useful. It is however this radical character that can be expected to result in unconventional reactivity as the metal strives to return to an even electron count dictated by the 18-electron rule. Complexes with Ru^{III}−alkyl bonds in particular are rare, principally due to considerably weaker, with respect to homolytic cleavage, Ru−C bonds (in comparison to their divalent congeners). This is exemplified by the one-electron oxidation of stable ruthenium(II) alkyls to Ru^{III}, resulting in rapid Ru−alkyl bond homolysis producing Ru^{II} products.[2−5] Recently, Gunnoe et al. have quantified by DFT calculations the effect that one-electron oxidation of TpRu(CO)(NCMe)Me has on the Ru−CH$_3$ homolytic bond dissociation enthalpy, discovering a dramatic (25.4 kcalmol^{-1}) decrease on oxidation.[2] Extensive studies by Tilset et al. also revealed the propensity on oxidation of CpRu(L)$_2$X (L = 2 electron neutral ligand X = H or Me) to undergo rapid Ru−X bond homolysis.[3,6−8] This predisposition to bond homolysis has even proved useful in oxidatively induced intermolecular reactions.[8,9]

$$L_nRu^{II}-R \xrightarrow{-e} [L_nRu^{III}-R] \xrightarrow{\text{homolysis}} L_nRu^{II} + R^{\bullet}$$

The instability of the Ru^{III}−R bond is further highlighted in the anionic Ru^{III} dialkyl complex [Ru(OEP)(CH$_3$)$_2$]$^-$ (OEP = octaethylporphyrin), which has a lifetime of only 500 μs, decaying via rapid methyl radical loss to produce divalent [Ru(OEP)(CH$_3$)(THF)]$^-$.[4] On moving up the triad to the more extensively studied Fe^{III} systems, similar reactivity is well documented, with Fe^{III} alkyl complexes prone to undergo fragmentation to produce alkyl radicals.[10−13] Indeed, the behavior of both Ru^{III} and Fe^{III} alkyls is highly reminiscent of the intensively studied Co-alkyl complexes that serve as models for vitamin B$_{12}$.[14−16] In a process related to M−C bond homolysis following one-electron oxidation of a monoalkyl L$_n$M−R complex, d^6 dialkyl L$_n$MR$_2$ complexes on oxidation commonly undergo reductive elimination to produce the coupled R−R product. This is a reaction best developed for the d^6 complexes (bipy)$_2$FeR$_2$ and Cp*M(PR$_3$)R$_2$ (M = Rh or Ir).[17−21]

A limited number of stable Ru^{III} alkyls have been successfully synthesized, though all are based on the redox-active porphyrinate dianion.[22−24] Employing the Ru^{III} poryphrinato framework has to the best of our knowledge been the only successful method for isolating complexes with stable Ru^{III}−R bonds and has even allowed for the crystallographic characterization of several.[23,24] As illustrated by the Ru^{III} porphyrin systems,

* To whom correspondence should be addressed. E-mail: caulton@indiana.edu.

(1) *Mononuclear Complexes of Ruthenium and Osmium Containing η^1-Carbon Ligands*; Hill, A. F., Ed.; Comprehensive Organometallic Chemistry II, Vol. 7; Shriver, D. F., Bruce, M. I., Eds.; Chapter 6, pp 299−441.
(2) Lail, M.; Gunnoe, B. T.; Barakat, K. A.; Cundari, T. R. *Organometallics* **2005**, *24*, 1301−1305.
(3) Aase, T.; Tilset, M.; Parker, V. D. *J. Am. Chem. Soc.* **1990**, *112*, 4794−4795.
(4) Seyler, J. W.; Safford, L. K.; Fanwick, P. E.; Leidner, C. R. *Inorg. Chem.* **1992**, *31*, 1545−1547.
(5) Collman, J. P.; Rose, E.; Venburg, G. D. *J. Chem. Soc., Chem. Commun.* **1994**, 11−12.
(6) Ryan, O. B.; Tilset, M.; Parker, V. D. *Organometallics* **1991**, *10*, 298−304.
(7) Ryan, O. B.; Tilset, M. *J. Am. Chem. Soc.* **1991**, *113*, 9554−9561.
(8) Smith, K. T.; Romming, C.; Tilset, M. *J. Am. Chem. Soc.* **1993**, *115*, 8681−8689.
(9) Ceccanti, A.; Diversi, P.; Ingrosso, G.; Laschi, F.; Lucherini, A.; Magagna, S.; Zanello, P. *J. Organomet. Chem.* **1996**, *525*, 251−262.
(10) Balch, A. L.; Olmstead, M. M.; Safari, N.; St. Claire, T. N. *Inorg. Chem.* **1994**, *33*, 2815−2822.
(11) Arasasingham, R. D.; Balch, A. L.; Latos-Grazynski, L. *J. Am. Chem. Soc.* **1989**, *111*, 4357−4363.
(12) Riordan, C. G.; Halpern, J. *Inorg. Chim. Acta* **1996**, *243*, 19−24.
(13) Tilset, M.; Fjeldahl, I.; Hamon, J.-R.; Hamon, P.; Toupet, L.; Saillard, J.-Y.; Costunas, K.; Haynes, A. *J. Am. Chem. Soc*. **2001**, *123*, 9984−10000.
(14) Halpern, J.; Kim, S.-H.; Leung, T. W. *J. Am. Chem. Soc.* **1984**, *106*, 8317−8319.
(15) Halpern, J. *Science* **1985**, *227*, 869−875.
(16) Jensen, M. P.; Zinkl, D. M.; Halpern, J. *Inorg. Chem*. **1999**, *38*, 2386−2393.
(17) Lau, W.; Huffman, J. C.; Kochi. *Organometallics* **1982**, *1*, 155−169.
(18) Pedersen, A.; Tilset, M. *Organometallics* **1993**, *12*, 56−64.
(19) Pedersen, A.; Tilset, M. *Organometallics* **1994**, *13*, 4887−4894.
(20) Fooladi, E.; Graham, T.; Turner, M. L.; Dalhus, B.; Maitlis, P. M.; Tilset, M. *Dalton Trans.* **2002**, 975−982.
(21) Diversi, P.; Iacoponi, S.; Ingrosso, G.; Laschi, F.; Lucherini, A.; Pinzino, G.; Uccello-Barretta, G.; Zanello, P. *Organometallics* **1995**, *14*, 3275−3287.

10.1021/om0508536 CCC: $33.50
Publication on Web 01/20/2006

Scheme 1. Lewis Acidic Nature of Four-Coordinate PNPRuMe

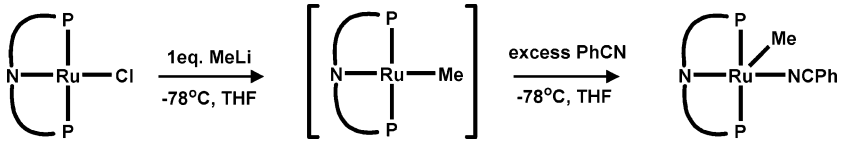

electron-deficient, radical metal centers can be stabilized by utilizing a bulky, electron-rich multidentate ligand. This principle has recently been successfully applied to synthesize a novel non-heme (and, importantly for the unambiguous determination of metal oxidation state, redox-innocent pincer ligands) Ru^{III} complex.[25] The utilization of a derivative of the bulky PNP pincer ligand (PNP = $(^tBu_2PCH_2SiMe_2)_2N^-$) initially developed by Fryzuk has led to the isolation of an unusual Ru^{II} complex, PNPRuCl, that is planar, low-coordinate (4), and highly unsaturated (formally only 14*e*).[26] Furthermore (Scheme 1), recent studies on PNPRuX (X = CH_3 or Cl) have demonstrated the metal center's ability to readily accept one or two additional uncharged Lewis bases (L).[26,27] This suggests that the formation of anionic complexes of the general formula $[PNPRu(X)Me]^-$ is feasible, and these subsequently (due to the strong electron-donating nature of the PNP ligand) may undergo one-electron oxidation.

Herein, we report the synthesis of a novel five-coordinate Ru^{III} dialkyl complex, $PNPRuMe_2$, that is stable with respect to Ru−C homolysis, its characteristic reactivity, and the synthesis of the related complex, $PNPRuI_2$.

Results and Discussion

Synthesis and Characterization of $PNPRuMe_2$. The addition of an excess (ca. 3 equiv) of MeLi to PNPRuCl at −78 °C in THF resulted in a rapid color change from yellow to brown. Immediate addition of excess CH_2Cl_2 at this temperature produced a vermillion solution. Removal of solvent and recrystallization from minimum pentane led to vermillion crystals in good yield, whose ^1H NMR spectrum revealed four new paramagnetically shifted peaks which exhibit drastically increased peak widths compared to triplet ($S = 1$) ground state starting material PNPRuCl. The ^1H NMR spectrum implies C_{2v} symmetry. The solution magnetic moment (Evans method, 298 K)[28,29] of 1.70 μ_B is consistent with a low-spin Ru^{III} complex. An X-ray diffraction study (Figure 1) on these vermillion crystals allowed for unambiguous identification as the five-coordinate, trivalent Ru compound $PNPRuMe_2$, **1**. The fourth observed ^1H NMR resonance can thus be attributed to the two Ru-Me groups that are equivalent in solution at 25 °C.

The structure of **1** is approximately a square-based pyramid with meridonal PNP ligand coordination. One methyl is occupying the axial position *trans* to the vacant site, and the other is located *trans* to the amide. As expected, comparison of the respective Ru−CH_3 bond distances reveals that the axial Ru−C bond length is the shorter. An agostic interaction in the sixth coordination site can be precluded, with the closest Ru−C (to a ^{t}Bu methyl) distance at 3.16 Å. Similarly, no α-agostic interactions associated with C23 are observed. The short Ru−N1 distance (2.124(2) Å) in comparison to known longer amine $P_2N(H)$−Ru bond lengths (e.g., 2.380(2) and 2.230(3) Å)[30,31] and the planar (angles around N sum to 358.8°) geometry is fully consistent with an amide functionality, supporting a formal ruthenium oxidation state of +3. The axial Ru−C bond length in **1** (2.075(2) Å) is comparable to the five-coordinate Ru^{III} porphyrin complex Ru(OEP)(neopentyl) (2.069 Å),[24] where neopentyl likewise is *trans* to a vacant site and also to the homoleptic Ru alkyl, $Ru_2(CH_2{}^tBu)_6$ (from 2.023(2) to 2.051(9) Å).[32] Interestingly, the longer Ru−C23 bond length (2.149(3) Å) in stable **1** is effectively identical to that calculated for the transient Ru^{III} complex $[TpRu(CO)(NCMe)Me]^+$ (2.14 Å), where rapid Ru−C bond homolysis occurs.[2] The square pyramidal geometry of **1** is in contrast to trigonal bipyramidal structures for the crystallographically determined Fe^{III} complexes, $PNP^{Ph}FeBr_2$ ($PNP^{Ph} = (Ph_2PCH_2SiMe_2)_2N^-$),[33] $FeBr_3(PPhMe_2)_2$,[34] $FeCl_3(PPh_3)_2$, and $FeCl_3(PMe_3)_2$,[35] though these all have a different electronic structure (spin states of $S = 5/2$ or $S = 3/2$) from **1**. The absence of any non-heme solid-state structures of five-coordinate Ru^{III} complexes (to the best of our knowledge) led us to synthesize $PNPRuI_2$, **2**, via the route outlined in Scheme 2, to allow for the direct comparison of electronic and solid-state properties.

Complex **2** also exhibits C_{2v} symmetry in solution (by ^1H NMR) and has three paramagnetically broadened and shifted resonances analogous to **1**. A low-spin d^5 ruthenium electronic

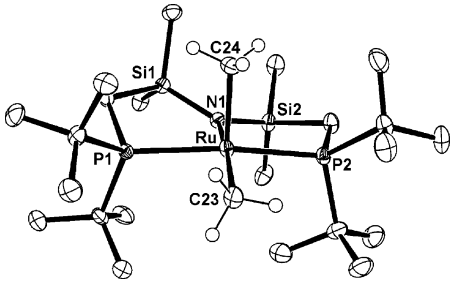

Figure 1. ORTEP view of **1** (50% probability ellipsoids). all hydrogen atoms apart from those on the Ru-methyls are removed for clarity. Selected bond lengths (Å) and angles (deg): Ru−C24: 2.075(2); Ru−C23: 2.149(3), Ru−N1: 2.124(2); Ru−P1: 2.3826(7); C24−Ru−N1: 91.49(10); N1−Ru−C23: 168.68(10), C24−Ru−C23: 99.75(11); P1−Ru−P2: 170.14(2).

(22) Collman, J. P.; McElwee-White, L.; Brothers, P. J.; Rose, E. *J. Am. Chem. Soc.* **1986**, *108*, 1332.
(23) Ke, M.; Rettig, S. J.; James, B. R.; Dolphin, D. *J. Chem. Soc., Chem. Commun.* **1987**, 1110−1112.
(24) Alexander, C. S.; Rettig, S. J.; James, B. R. *Organometallics* **1994**, *13*, 2542−2544.
(25) Arnold, P. L.; Scarisbrick, A. C. *Organometallics* **2004**, *23*, 2519−2521.
(26) Watson, L. A.; Ozerov, O. V.; Pink, M.; Caulton, K. G. *J. Am. Chem. Soc.* **2003**, *125*, 8426−8427.
(27) Ingleson, M. J.; Yang, X.; Pink, M.; Caulton, K. G. *J. Am. Chem. Soc.* **2005**, *127*, 10846−10847.
(28) Evans, D. F. *J. Chem. Soc.* **1959**, 2003−2005.
(29) Sur, S. K. *J. Magn. Reson.* **1989**, *82*, 169−173.
(30) Fryzuk, M. D.; Montgomery, C. D.; Rettig, S. J. *Organometallics* **1991**, *10*, 467−473.
(31) Walstrom, A.; Pink, M.; Tsvetkov, N. P.; Fan, H.; Ingleson, M. J.; Caulton, K. G. *J. Am. Chem. Soc.* **2005**, *127*, 16780−16781.
(32) Tooze, R. P.; Motevalli, M.; Hursthouse, M. B.; Wilkinson, G. *J. Chem. Soc., Chem Commun.* **1984**, 799−800.
(33) Fryzuk, M. D.; Leznoff, D. B.; Ma, E. S. F.; Rettig, S. J.; Young, V. G., Jr. *Organometallics* **1998**, *17*, 2313−2323.
(34) Godfrey, S. M.; Kelly, D. G.; Mackie, A. G.; MacRory, P. P.; McAuliffe, C. A.; Pritchard, R. G.; Watson, S. M. *J. Chem. Soc., Chem. Commun.* **1991**, 1447−1449.
(35) Walker, J. D.; Poli, R. *Inorg. Chem.* **1989**, *28*, 1793−1801.

Scheme 2 Synthetic Route to Trivalent PNPRuI$_2$, 2, and (right) the ORTEP View (50% probability ellipsoids) of Only One of Three Independent Molecules of 2[a]

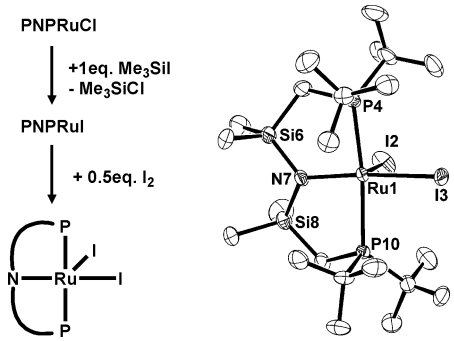

[a] Hydrogen atoms and a molecule of lattice solvent are omitted for clarity.

configuration was confirmed by a magnetic moment of 2.18 μ_B (Evans method, 298 K).[28,29] Complex **2** crystallizes with three independent molecules in the unit cell, each possessing similar structural parameters. The geometry around ruthenium approximates to a square-based pyramid, as observed for **1**, but in contrast to the trigonal bipyramid Fe^{III} analogue, PNP^{Ph}-FeBr$_2$,[33] implying that the different geometries observed for five-coordinate Fe^{III} and the Ru^{III} complexes **1** and **2** are a direct consequence of the change in spin state. Correspondingly to that noted for **1**, the axial Ru−I bond (average = 2.64 Å) is noticeably shorter than the Ru−I bond *trans* to amide (average = 2.69 Å). The Ru−N bond lengths (2.043(3) to 2.089(4) Å) are also fully consistent with an amide functionality and support a ruthenium oxidation state of +3. The shorter Ru−amide bond in **2** compared to that in **1** presumably originates from the weaker *trans* effect of iodide. Again there is no evidence for any agostic interaction in **2**.

Both low-spin d^5 complexes **1** and **2** would be expected to have a rhombic EPR spectrum. This is the case for complex **1** when the X-band EPR spectrum is recorded in glassy toluene (77 K) (Figure 2; identical experimental spectra have been obtained from a number of independently synthesized batches of pure crystalline **1**), and the spectrum has been satisfactorily simulated. As well as the observed asymmetry (approximate g values $g_1 = 2.30$, $g_2 = 2.065$, and $g_3 = 2.045$) a number of hyperfine couplings are observed to both the two ^{31}P ($I = {}^1/_2$) nuclei and the single ^{14}N ($I = 1$) nucleus; significantly the simulated coupling to ^{14}N is highly anisotropic. No ^{1}H hyperfine coupling could be resolved, suggesting at most small spin densities on the methyl on Ru.

Interestingly, given the similar solid-state structure, the equally rhombic EPR spectrum for **2** at 77 K in glassy toluene

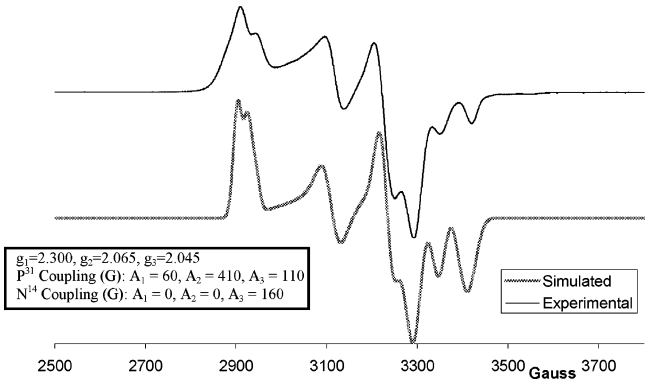

Figure 2. X band spectra of **1** in frozen toluene (77 K) and the simulated best fit spectra.

Figure 3. Possible resonance delocalization of the unpaired electron in **1**.

(see Supporting Information, approximate g values $g_1 = 2.51$, $g_2 = 2.28$, and $g_3 = 1.97$) is drastically different from that recorded for **1**, with no hyperfine coupling observed.

Compound **1** is thermally stable at 25 °C in hydrocarbon solvents under anaerobic conditions with no decomposition observed after 7 days, implying Ru−C bonds that are not prone to homolysis. The additional stability of **1** (and in particular the Ru−CH$_3$ bond) compared to other Ru^{III} alkyls may be in part due to an intramolecular electron transfer from the amide functionality to the metal center, forming a Ru^{II}-aminyl complex (Figure 3). This is supported in part by the observation of a highly anisotropic hyperfine coupling (160 G) to N in the EPR spectrum of **1**. As previously discussed for the [Rh^I(trop$_2$N$^•$)-(bipy)]$^+$ cation, a large anisotropy observed in the hyperfine coupling to N implies that in the aminyl structure the radical resides in an orbital of predominantly p character;[36] hence each resonance form of **1** shown in Figure 3 would have a planar geometry around nitrogen, fully consistent with the observed solid-state structure.

A conceptually related radical delocalization into the porphyrin framework (thereby making it formally Ru^{II}) could also contribute to the observed stability of "Ru^{III}" alkyls ligated by OEP. Furthermore, a similar intramolecular nitrogen-to-metal electron transfer has been recently reported in what is formally a Ni^{III}-imido species, [Me$_3$NN]Ni═NAd ([Me$_3$NN] = a bulky β diketiminate ligand), and again a highly anisotropic hyperfine coupling to ^{14}N is observed, consistent with the calculated SOMO (SOMO = singly occupied molecular orbital) having significant spin density on the imido nitrogen.[37] With no observable hyperfine coupling in the EPR spectrum of **2** an analogous electron transfer is unlikely, and the compound stability presumably is due to the stronger Ru−halogen bond.

The mechanism for the formation of **1** could be expected to proceed via a diamagnetic Ru^{II} complex of general formula PNPRuMe$_x$(Li•solv$_n$)$_{x-1}$ ($x = 2$ or 3), followed by oxidation with CH_2Cl_2. The primary product, observed following reagent combination at −70 °C (and before CH_2Cl_2 addition) in d_8-THF, is indeed diamagnetic, with a singlet observed in the ^{31}P{^{1}H} NMR spectrum (53.0 ppm), consistent with coordination number ≥5. The ^{1}H NMR spectrum at this temperature revealed a molecule with only C_s symmetry (determined by the observation of two inequivalent, 6H intensity, SiMe resonances) and an upfield singlet at −2.04 of integral 6 assigned to two ruthenium-bound methides. Due to the presence of excess *protio* Et_2O (from MeLi solution), no further information from this spectrum was obtainable. Above −40 °C this primary product reacts further to give a single cyclometalated product, preventing complete characterization of the primary product. Possible structures for this primary product are shown in Figure 4 and are related to that previously characterized as the low-temperature product on addition of excess MeLi to Ru(H)Cl(PPh$_3$)$_3$ in THF by Wilkinson et al.[38]

Consistently, the crude reaction mixture from the synthesis of **1** using CH_2Cl_2 as the oxidant contained a second minor

(36) Buttner, T.; Geier, J.; Frison, G.; Harmer, J.; Calle, C.; Schweiger, A.; Schonberg, H.; Grutzmacher, H. *Science* **2005**, *307*, 235−238.
(37) Kogut, E.; Wiencko, H. L.; Zhang, L.; Cordeau, D. E.; Warren, T. H. *J. Am. Chem. Soc.* **2005**, *127*, 11248−11249.
(38) Cole-Hamilton, D. J.; Wilkinson, G. *J. Chem. Soc., Dalton Trans.* **1977**, 797−804.

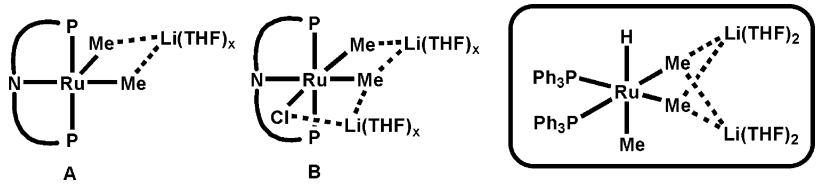

Figure 4. Two possible primary products from the addition of excess MeLi to PNPRuCl and, inset, the characterized product from the reaction of excess MeLi with $Ru(H)Cl(PPh_3)_3$.

paramagnetic product, even when the excess CH_2Cl_2 is removed in vacuo at low temperature. It equally appears to be a Ru^{III} product (by the observed three paramagnetically broadened and shifted resonances) and is C_{2v} symmetric in solution. This compound has been identified as the trivalent ruthenium complex PNPRuMe(Cl) on the basis of the full characterization of the single diamagnetic product from the reaction between PNPRuMe(Cl) and NO, namely, PNPRu(Me)(NO)Cl (see later discussion). The formation of PNPRu(Me)Cl could be envisaged to occur via two pathways: (i) oxidation of a Ru−Cl-containing compound (e.g., B, Figure 4) or the subsequent reaction of **1** with a radical byproduct (e.g., $^{\bullet}CH_2Cl$). Pure compound **1** does slowly react with CH_2Cl_2 (no **1** is detectable after 24 h at 25 °C) to produce a number of new Ru^{III} products, one of which is PNPRu(Me)Cl, but due to the poor overall yield and long reaction time required, CH_2Cl_2 is ruled out as the co-reactant in the low-temperature synthesis that produces PNPRu(Me)Cl. To improve the overall yield of **1** and to avoid the need for fractional recrystallization to separate **1** from PNPRu(Me)Cl, a number of alternative synthetic pathways were investigated. The reaction of **2** (cleanly synthesizable in high yield) with 2 equiv of MeLi at −78 °C in THF also led to a mixture of products, with **1** present only as a minor component. A number of alternative one-electron oxidants in place of CH_2Cl_2 were then tried, including a classic outer-sphere oxidant, ferrocenium (as the $[PF_6]^-$ salt), which did produce **1**, but again only in poor yield. An optimum synthesis using benzyl bromide as the one-electron oxidant was developed that produced **1** as the only Ru^{III} product observed in the crude mixture after removal of residual benzyl bromide at low temperature. Presumably the radical byproduct dimerizes to bibenzyl, thereby preventing any undesirable secondary reactions. Importantly, **1** slowly reacts with benzyl bromide in solution (over hours as with CH_2Cl_2), so in order to obtain pure, good yields of **1**, the removal of all remaining benzyl bromide is imperative. With an improved synthesis of **1** in hand its reactivity with radicals (to determine the predominant location of the radical character in **1**) and with even-electron reagents was investigated.

Reactivity Studies on $PNPRuMe_2$ (a) NO. The obvious route to generate a diamagnetic complex from a Ru^{III} compound is by the addition of another radical. Addition of excess NO to a benzene solution of **1** resulted on thawing in a rapid color change from vermillion to pale yellow. The NMR spectra confirmed the formation of a single diamagnetic product ($^{31}P\{^1H\}$ NMR resonance a singlet at 48.8 ppm) with C_s symmetry and two Ru-Me signals. The infrared spectrum (1715 cm^{-1}, pentane) is consistent with a linear NO^+ motif, resulting in an overall ruthenium oxidation state of +2, and is in a range similar to that reported for the closely related complex $Ru(H)_3(NO)(P^tBu_2Me)_2$ (1676 cm^{-1}), where NO is also *trans* to a strong σ donor ligand (hydride).[39] The expected thermodynamic product would be with NO *trans* to amide to maximize the push/pull interaction between π basic amide and π acidic NO; this

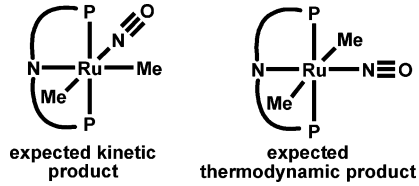

Figure 5. Two possible Ru^{II} products resulting from the addition of NO to compound **1**.

however would be expected in solution to produce NMR spectra consistent with C_{2v} symmetry. The lower symmetry observed (i.e., inequivalent Ru-methyls) leads to the assignment as the kinetic product (left, Figure 5), $PNPRuMe_2NO$, **3**, with one methide *trans* to amide and the other *trans* to the NO. The presence of two drastically different methide *trans* environments is supported by the disparity in the chemical shifts of the two methides (^1H NMR, 1.43 and 0.90 ppm). On heating, **3** does not convert to the expected thermodynamic product even after 7 days at 65 °C, with compound **3** recovered unchanged.

The formation of the Ru^{II} product with linear NO over the Ru^{IV} product with bent NO indicates that, despite the highly electron-donating nature of the PNP ligand, the lower Ru oxidation state is still thermodynamically favored. The addition of radical NO to the ruthenium center instead of to the ligand nitrogen in the kinetic product suggests that the Ru^{III}-amide resonance structure dominates over the Ru^{II}-aminyl structure.

The addition of NO gas was utilized further to identify the second paramagnetic compound consistently observed in the synthesis of **1** when CH_2Cl_2 is the oxidant. Following addition of NO to the crude mixture of **1** two diamagnetic products were observed ($^{31}P\{^1H\}$, 48.8 and 50.9 ppm). The major diamagnetic product observed is **3**. In solution the second complex also has C_s symmetry, and due to its lower solubility in low dielectric solvents compared to **3** (by methide for chloride exchange), a small number of pale yellow crystals were obtainable by fractional recrystallization. The ^1H NMR spectrum on this isolated sample revealed only one intensity 3 triplet at 1.73 ppm, which we assign to a methide *trans* to NO, leaving the chloride *trans* to amide; again the kinetic product PNPRuMe(Cl)NO, **4**, is the only isomer observed. The infrared N−O stretching frequency at 1747 cm^{-1} again is fully consistent with a linear NO^+. An X-ray diffraction study (Figure 6) confirmed the anticipated formula and the assignment as the kinetic isomer with NO and methide respectively *trans*.

The structure of **4** is close to an ideal octahedron with the PNP ligand meridonal, chloride *trans* to amide, and methide and linear NO mutually *trans*. The NO and $C(23)H_3$ ligands are disordered with each other over the two axial sites; the structural metrics for both disordered parts are essentially identical, and only one will be discussed here. The six-coordinate, 18-electron nature of **4** forces a significant rotation of the trigonal planar Si_2N−Ru moiety away from the $P_2RuN(Cl)$ equatorial plane (dihedral angles: P2−Ru−N1−Si1 = 145.66(12)°, P1−Ru−N1−Si2 = 148.31(12)°). This twist would orient the amide lone pair away from an occupied ruthenium/

(39) Huang, D.; Streib, W. E.; Eisenstein, O.; Caulton, K. G. *Organometallics* **2000**, *19*, 1967−1972.

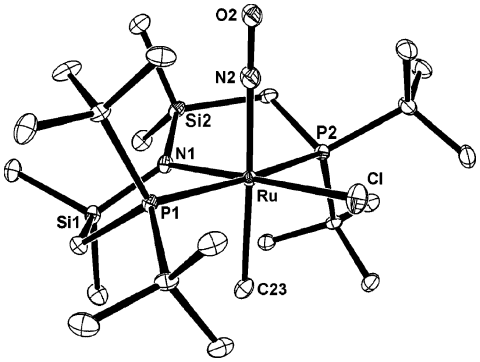

Figure 6. ORTEP view of **4**. Hydrogen atoms and disorder (of methyl carbon C23 with NO) are removed for clarity (thermal ellipsoids are shown at the 50% probability level). Selected bond lengths (Å) and angles (deg): Ru−C23: 2.090(10); Ru−N2: 1.873(9); N2−O2: 1.126(10); Ru−N1: 2.112(2); Ru−P1: 2.4808(7); P1−Ru−P2: 171.46; C23−Ru−N1: 88.8(4); C23−Ru−N2: 177.1(4): Ru−N2−O2: 177.6(12).

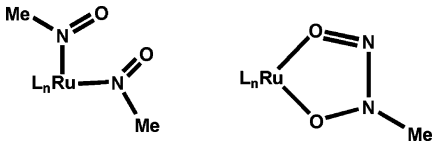

Figure 7. Possible insertion products expected in the reaction between **1** and excess NO.

ligand orbital, thereby reducing electron−electron repulsion by interacting less with one of the filled dπ orbitals conjugated with the NO ligand. The linear NO motif has a longer Ru−N bond but a similar N−O bond length when compared to the related octahedral $RuCl_3(NO)(PPh_3)_2$ (Ru−N = 1.737(7) Å and N−O = 1.142(8) Å), where the two phosphines are equally in a *trans* arrangement.[40] Curiously, the NO stretching frequency for $RuCl_3(NO)(PPh_3)_2$ (1881 cm^{-1}) is significantly higher than that observed for **3** and **4** and is in apparent disagreement with the respective solid-state N−O distances. However when **4** is compared to the related Ru(0) complex $Ru(CH_3)(NO)(P^iPr_3)_2$ (also with bulky electron-donating phosphines, and where the linear NO is equally *trans* to methide), then there is a better correlation between solid-state N−O distance and infrared stretching frequency (Ru−N = 1.823(12) Å, N−O = 1.059 Å, ν(N−O) = 1661 cm^{-1}).[39] Care has to be taken not to overinterpret these solid-state metrics with the parameters involved disordered in **4**, though it is unambiguous that the NO moiety does not deviate significantly from linearity.

It is noteworthy in the reactivity of **1** with NO that there is no coupling of NO and the methide ligands to form either coordinated RNO or the *N*-nitrosoaminohydroxide ligand (Figure 7), the latter occurring (twice) with the highly unsaturated molecule WMe_6.[41] Presumably the 18-electron character of **3** and **4** discourages insertion and subsequent addition of NO.

(b) H Atom Abstraction, Addition, or Electron Transfer. In a further attempt to locate the maximum spin density in **1**, a number of other reactions involving H atom donors and radical reagents were investigated. Radicals are well documented to abstract a hydrogen atom from a reagent with a weak X−H bond, and recently there has been a number of successes in organometallic complexes with nitrogen-based radicals reacting

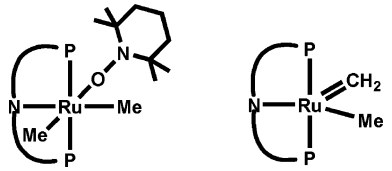

Figure 8. Potential products from reaction between **1** and TEMPO.

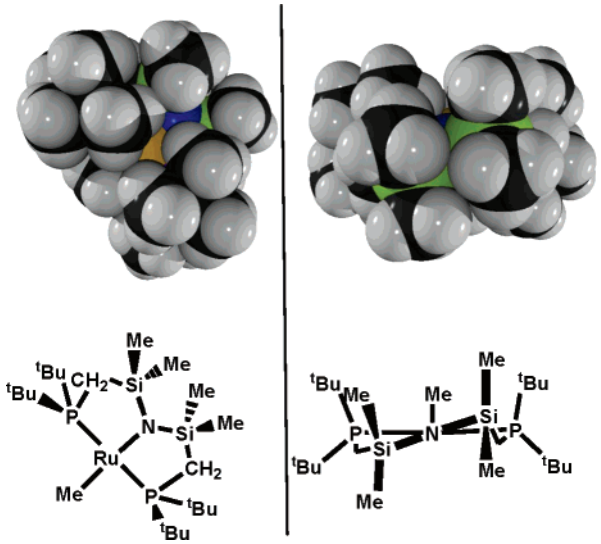

Figure 9. (Top) Space-filling diagrams of **1**, left, down the vacant axial site−Ru−Me−axis and, right, down the N−Ru−C axis. Green = Si, blue = N, orange = Ru, dark gray = carbon, light gray = hydrogen. (Bottom) Schematic representations at approximately the same orientation.

in this manner.[36,37,42] Hoping for a similar outcome, **1** was reacted with stoichiometric equivalents of $^nBu_3SnH$ and 9,10-dihydoranthracene at 25 °C. In both cases no reaction was observed after 24 h (**1** was recovered unchanged). While heating a sample of **1** and stoichiometric $^nBu_3Sn$−H to 60 °C did result in the complete disappearance of resonances assignable to **1**, only an intractable mixture containing numerous products (vide infra) was formed. The addition of TEMPO (TEMPO = 2,2,6,6-tetramethyl-1-piperidinyloxyl radical) was attempted to form either a direct Ru-TEMPO nitroxyl adduct or to abstract a hydrogen atom from a Ru−Me, thereby forming a Ru=CH_2 group (Figure 8); again however, no reaction was observed. The lack of any H atom abstraction from a Ru−CH_3 group by TEMPO suggests a strong C−H bond, with no significant weakening of the Ru−Me C−H bond by the radical in **1**. It is also consistent with no resolved hyperfine coupling to these hydrogens.

In a related manner the reaction between **1** and radical Cp_2Co (cobaltocene) was attempted, likewise without success. In both cases, the failure of two radicals to react initially seems strange, but the stability of **1** here to bimolecular reactions arises from its extensive steric protection, with a reaction observed only with the small NO radical. This is made apparent by the examination of the space-filling diagram for **1** (Figure 9), which reveals that the radical (be it predominantly N- or Ru-based) is encapsulated by the bulky hydrocarbon periphery, preventing the close approach of all but the smallest molecules. With this in mind the successful one-electron oxidation of the anionic intermediate ("$[PNPRuMe_2]^-$") by benzyl bromide to form **1** has the appearance of an outer-sphere electron transfer process

(40) Haymore, B. L.; Ibers, J. A. *Inorg. Chem.* **1975**, *14*, 3060−3070.
(41) Fletcher, S. R.; Shortland, A.; Skapski, A. C.; Wilkinson, G. *J. Chem. Soc., Chem. Commun.* **1972**, 992.
(42) Lucas, R. L.; Powell, D. R.; Borovik, A. S. *J. Am. Chem. Soc.* **2005**, *127*, 11596−11597.

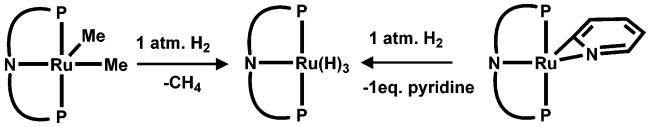

Figure 10. Two alternative routes for the synthesis of PNPRu-$(H)_3$, **5**.

(i.e., no Ru−halogen bond formation); this is a reaction less subject to steric inhibition than atom transfer.

(c) H_2. The reactivity of **1** with respect to even-electron reagents (with the knowledge in hand that only small molecules would have the potential to reach the radical core) was next investigated. The addition of an excess of H_2 to **1** ultimately produces one new diamagnetic product and methane (confirmed by the observation of CH_3D with the use of D_2). The diamagnetic product ($^{31}P\{^1H\}$ at 84.8 ppm) possesses C_{2v} symmetry and has an intensity 3 hydride resonance as a triplet centered at −15.1 ppm ($^2J_{P-H} = 14$ Hz); this is assigned as the polyhydride PNPRu$(H)_3$, **5**, on the basis of the close spectroscopic similarity and analogous reactivity to previously synthesized PNP^{Cy}Ru$(H)_3$ (PNP^{Cy} = $(Cy_2PCH_2SiMe_2)_2N$).[43] The product from the reaction of **1** and D_2 produces an identical NMR apart from the complete lack of any hydride resonance, confirming all hydrides in **5** originate from dihydrogen. Compound **5** can also be independently synthesized from the reaction of H_2 with the previously reported[27] compound PNPRu-(η^2-NC_5H_4), concomitantly generating an equivalent of pyridine (Figure 10).

Immediate monitoring of the reaction between **1** and 1 atm of H_2 at 22 °C (C_6D_6) reveals an observable intermediate complex present in low concentration (along with NMR resonances attributable to **1** and **5**) that has ^1H NMR line widths consistent with a low-spin d^5 Ru^{III} center. This is supported by the lack of any observable resonance in the $^{31}P\{^1H\}$ NMR (other than that of **5**). Only three new resonances are observed assignable to this intermediate in the ^1H NMR spectrum, suggesting that it is PNPRu$(H)_2$ (though PNPRu(Me)H is also a feasible product, with the fourth proton environment (Ru−Me) not observed due to its low concentration and the large peak width that would be associated with this resonance). Conversion from trivalent PNPRu$(H)_2$ to diamagnetic PNPRu-$(H)_3$ would then occur via some atom transfer process, which would be expected to be slower. The fact that there is no product observed containing an amine functionality strongly suggests that in PNPRuH_2, at least, the radical is Ru^{III}-based.

(d) CO. Moving to a small diamagnetic molecule that cannot undergo bond cleavage, the addition of excess CO to **1** was investigated. This also resulted in a rapid color change to pale yellow. The NMR spectrum now revealed a single diamagnetic product ($^{31}P\{^1H\}$ singlet, 68.7 ppm) with solution C_s symmetry. The infrared spectrum revealed two resonances at 1920 and 1633 cm^{-1} (pentane), consistent with metal-carbonyl and metal-acyl groups. The acyl corresponds to an intensity 3 singlet in the ^1H NMR spectrum shifted downfield to 2.82 ppm. The mass spectrum revealed the expected molecular ion peak for PNPRu-(COMe)CO (M + 1, ESI) at 662.4 *m/z*. These data combined with comparison to the related structure ($^tBu_2PCH_2SiMe_2$)N(Me_2-$SiCH_2P^tBuCMe_2CH_2$(CO))RuCO led us to characterize this new product as PNPRu(COMe)CO, **6** (Figure 11).[27] Due to the similarities in the infrared stretching frequencies between **6** and ($^tBu_2PCH_2SiMe_2$)N($Me_2SiCH_2P^tBuCMe_2CH_2$(CO))RuCO, it is reasonable to assume that the acyl moiety occupies the axial

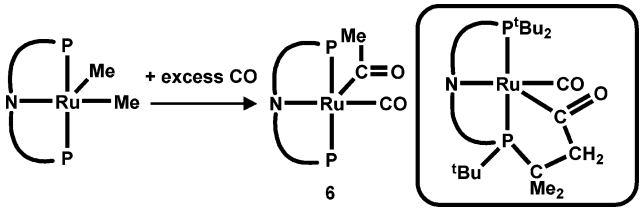

Figure 11. Synthesis of PNPRu(CO)(COMe), **6**, and (right) the closely related complex ($^tBu_2PCH_2SiMe_2$)N($Me_2SiCH_2P^tBu$(CO)-CH_2CMe_2)RuCO.

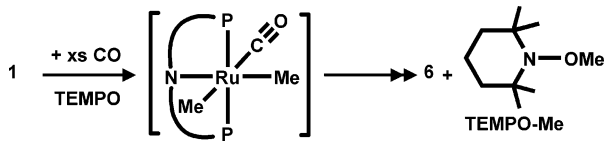

Figure 12. Synthesis of **6** in the presence of TEMPO via the expected intermediate, PNPRu$(Me)_2$CO.

position, while the CO is *trans* to the amide, resulting in the thermodynamically preferred structure. The assignment of **6** based on spectroscopic data is corroborated by an imperfect X-ray diffraction study (see Supporting Information), which supports a square pyramidal structure with CO *trans* to amide and acyl in the axial position as expected. Any further discussion of the structural metrics is not warranted due to the poor data set.

The presence of only one methyl in complex **6** suggests a reaction mechanism involving a homolytic cleavage of a Ru−alkyl bond, as observed in related six-coordinate Ru^{III}-CH_3 species.[2] Analysis of the volatile products from the formation of **6** revealed only the presence of ethane; no acetone or biacetyl was observed (by ^1H NMR). To further corroborate the loss of $^{\bullet}CH_3$ from **1**, the reaction was repeated in the presence of TEMPO as a radical-trapping agent. An identical $^{31}P\{^1H\}$ NMR chemical shift was observed along with ^1H NMR resonances attributable to **6**. In addition 1 equiv of TEMPO-Me (3H intensity singlet at 3.6 ppm, Figure 12)[44] was also observed, confirming the trapping of a stoichiometric quantity of methyl group by TEMPO in the formation of **6**. The initial step presumably involves the coordination of CO to the vacant coordination site in **1**, generating a six-coordinate intermediate. This initial CO coordination can be envisaged to decrease the bond dissociation energy of one of the two Ru-CH_3 (presumably the *trans* to CO methide), permitting methyl transfer. The five-coordinate nature of **1** may therefore also be a significant factor in its unusual stability; this is supported by the short Ru−Me_{axial} bond length (2.075(2) Å) in the solid-state structure of **1**.

Contrastingly, the addition of stoichiometric (or excess) PhCN (a Lewis base of low steric profile known to be able to "penetrate" the bulky PNP ligand periphery) to a solution of **1** resulted in no reaction. The previously characterized expected product (assuming Ru−CH_3 homolysis) PNPRu(PhCN)Me was not observed even after 7 days at 25 °C. This could be attributable to the increased steric environment on moving from "monomethyl" PNPRuMe to "dimethyl" PNPRuMe_2, preventing PhCN coordination. Alternatively if the incoming ligand and the amide lone pair bonding interaction involve the same metal-based orbital, then the weaker donor PhCN (in comparison to CO) may now be thermodynamically unfavorable with respect to the multiple-bonding character between N and Ru. The *trans*

(43) Watson, L. A.; Coalter, J. N., III; Ozerov, O.; Pink, M.; Huffman, J. C.; Caulton, K. G. *New J. Chem.* **2003**, *27*, 263−273.

(44) Whitesides, G. M.; Newirth, T. L. *J. Org. Chem.* **1975**, *40*, 3448−3450.

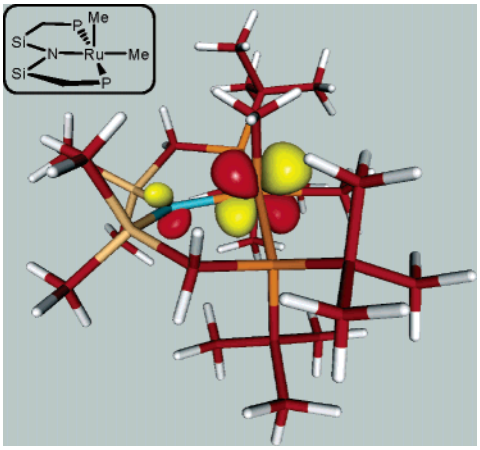

Figure 13. Orbital contour diagram for the calculated SOMO of the full model of compound **1**. Inset: schematic of the core atoms of **1** in an identical orientation.

influence of methyl may also be influential here. To gain further insight into the nature of the SOMO, and to test the conclusion based on experimental results (i.e., the radical character being seemingly predominantly metal-based), DFT calculations were performed on **1**.

DFT Calculations. Shown in Figure 13 is an orbital contour diagram of the SOMO calculated at the equilibrium geometry from an unrestricted wave function DFT calculation for the full molecule, $[(^tBu_2PCH_2SiMe_2)_2N]RuMe_2$. The calculated geometry (see Supporting Information) is close to the observed solid-state structure found for **1**, with comparable angles around ruthenium and the shorter apical Ru−Me reproduced.

The orbital contour diagram at the above geometry shows the SOMO to be Ru/N π antibonding and to have considerable N p−π orbital character (consistent with the observed anisotropy in the hyperfine coupling to N). The spin density of the SOMO is 84% on Ru and 8% on the amide nitrogen p−π orbital; the remaining spin density is distributed among other atoms, with none having a spin density greater than 1.6%. This degree of delocalization of the oxidation away from the metal to the amide N makes classifying the ruthenium in **1** as "Ru^{III}" an oversimplification, while simultaneously helping to explain the thermal stability of **1**. The radical character is not significant at any methide (thus C−H bonds that are not weakened) and also does not affect the Ru−CH_3 σ bonds (therefore no Ru−C homolysis at 25 °C). The antibonding character inherent in the SOMO (and hence its energy) is reduced to a degree by the significant twisting of the Si−N−Si backbone observed in the solid-state structure of **1** that somewhat reorients the amide lone pair away from the metal-based orbital. Presumably without the constraints imposed by the chelate nature of the PNP ligand, the amide would rotate further to position its lone pair perpendicular to the metal-based orbital, which would result in a nonbonding SOMO. Furthermore with the majority of the radical character calculated to be associated with the metal center, the lack of any observable reactivity at the amide functionality is not surprising.

Conclusions

The unusual stability of the Ru^{III} dialkyl complex **1** has been attributed by a combination of spectroscopic methods, reactivity patterns, and DFT calculations to a number of synergic effects: (i) the steric protection offered by the bulky PNP ligand; (ii) the noninnocence of the ligand environment, with the potential for intramolecular electron transfer from the amide functionality, formally reducing the ruthenium oxidation state (and thereby increasing the Ru−CH_3 homolytic bond dissociation energy); (iii) the low coordination number of **1**, specifically resulting in a short $Ru-Me_{axial}$ bond.

The contribution of the aminyl resonance form postulated for $PNPRuMe_2$ (and supported by the DFT calculations of the SOMO) would be in accord with the electron-rich character of the anionic PNP ligand, which, along with the ruthenium metal in the anion "$[PNPRuMe_2]^-$", becomes the locus of one-electron oxidation. The chemistry observed for **1** shows coupling to small radicals (i.e., NO) and a tendency to find a path to even-electron (16/18 electron) products with the nonradical reagents H_2 and CO (the latter formally reducing Ru, even though CO is not commonly considered a reducing agent). We were surprised that there is no tendency toward the loss of ethane by reductive coupling from **1** (though this may be disfavored by the expected product requiring a Ru^I oxidation state) or to form acetone (or a related $^{\bullet}CH_3$ to CO migration product) in the reaction with CO. Finally, H atom abstraction by TEMPO from a sterically accessible Ru-Me group to form diamagnetic $PNPRu(=CH_2)$-Me does not occur, suggesting that the radical character in **1** does not significantly weaken these C−H bonds.

Experimental Section

General Considerations. All manipulations were performed using standard Schlenk techniques or in an argon-filled glovebox. Solvents were distilled from Na/benzophenone, CaH_2, or 4 Å molecular sieves, degassed prior to use, and stored in airtight vessels. All reagents were used as received from commercial vendors. $[(^tBu_2PCH_2SiMe_2)_2N]RuCl$ was prepared according to the literature procedure.[23] ^1H NMR chemical shifts are reported in ppm relative to protio impurities in the deuterated solvents. $^{31}P\{^1H\}$ spectra are referenced to external standards of 85% H_3PO_4 (at 0 ppm). NMR spectra were recorded with a Varian Gemini 2000 (300 MHz ^1H; 121 MHz ^{31}P; 75 MHz ^{13}C) or a Varian Unity Inova instrument (400 MHz ^1H; 162 MHz ^{31}P). Infrared spectra were recorded on a Nicolet 510P FT-IR spectrometer. EPR spectra were obtained on a Bruker 300ESP spectrometer operating at X-band (ca. 9.4 GHz): microwave power, 2 mW; modulation amplitude, 1.0 G, modulation frequency, 100 kHz; receiver gain, 1.00×10^4. All EPR spectra were observed in toluene as frozen glasses at 77 K. The values of unresolved coupling ($A = 5.2$ G) are derived from the fitting program and are thus less accurate.

$PNPRuMe_2$, 1. A Schlenk flask was charged with PNPRuCl (0.200 g, 0.34 mmol), dissolved in 10 mL of THF, and cooled to −78 °C. Three equivalents of MeLi solution (0.64 mL, 1.02 mmol) was added dropwise at this temperature, resulting in a rapid color change from yellow to brown, via red (previously reported) PNPRuMe.[24] The solution is stirred at this temperature for 5 min before 3.1 equiv of benzyl bromide is added (0.126 μL, 1.05 mmol). On stirring at −78 °C the solution rapidly turns vermillion, and the solvent is then removed in vacuo at low temperature. The vermillion oil is redissolved in 10 mL of pentane, filtered, reduced to minimum volume, and stored at −40 °C overnight, yielding 0.154 g (0.271 mmol) of vermillion crystals. Yield: 80%. ^1H (298 K, C_6D_6): 15.30 (v br s), 7.40 (v br, s), −0.26 (br, s), and −11.80 (v br, s). Despite repeated attempts, reliable integration was not obtainable, presumably due to the large peak widths at half-intensity (>300 Hz) for a number of the resonances. Magnetic moment (Evans method, 298 K): 1.70 μ_B. EPR spectrum (77 K, frozen toluene, values from simulated spectrum): $g_1 = 2.300$, $g_2 = 2.065$, $g_3 = 2.045$. P^{31} coupling (G): $A_1 = 60$, $A_2 = 410$, $A_3 = 110$. N^{14} coupling (G): $A_1 = 0$, $A_2 = 0$, $A_3 = 160$.

PNPRuI. A Schlenk flask was charged with PNPRuCl (0.120 g, 0.21 mmol), which was dissolved in 5 mL of toluene. Then 1.1 equiv of Me_3SiI (0.23 mmol, 32 μL) was added dropwise, resulting

in an immediate color change to orange. The solvent and excess Me_3SiI were then removed in vacuo to leave 0.114 g (0.17 mmol) of an analytically pure microcrystalline orange solid. Yield: 83%. ^1H (298 K, C_6D_6): 30.43 (s, 12H), −13.56 (s, 36H), and −40.10 (s, 4H). Magnetic moment (Evans method, 298 K): 3.28 μ_B.

PNPRuI$_2$, 2. A Schlenk flask was charged with PNPRuI (0.050 g, 0.074 mmol), which was dissolved in 5 mL of toluene. Half an equivalent of I_2 (0.009 g, 0.037 mmol) was dissolved in 5 mL of toluene and added dropwise over 15 min at room temperature. The solution darkened from orange to black over the addition. The solvent was then removed in vacuo to leave 0.048 g (0.06 mmol) of an analytically pure black oily solid. Yield: 81%. ^1H (298 K, C_6D_6): 12.76 (v br, s), −1.39 (br s), −20.70 (v br s). Magnetic moment (Evans method, 298 K): 2.18 μ_B. EPR spectrum (77 K, frozen toluene): $g_1 = 2.510$, $g_2 = 2.275$, $g_3 = 1.970$.

PNPRuMe$_2$(NO), 3. $PNPRuMe_2$ (0.040 g, 0.069 mmol) was loaded into a sealable tube with a Teflon valve and dissolved in 5 mL of THF. The solution was degassed three times using freeze/pump/thaw cycles, and 1 atm of NO was added to the frozen solution. On thawing, the solution rapidly changed color from vermillion to pale yellow. The solvent and excess NO were then removed in vacuo to leave a dark yellow oil; attempts to recrystallize this material to obtain solid material failed, though **3** is the only product observed. ^1H (298 K, C_6D_6): 1.44 (3H, t, J_{H-P} 3.6 Hz), 1.23 (18H, t, J_{H-P} 6 Hz), 1.22 (18H, t, J_{H-P} 6 Hz). 1.03 (4H, complex multiplet from two overlapping doublets of triplets), 0.91 (3H, t, J_{H-P} 11.2 Hz), 0.47 (6H, s) and 0.42 (6H, s). $^1H\{^{31}P\}$ (298 K, C_6D_6): 1.43 (3H, s), 1.23 (18H, s), 1.22 (18H, s), 1.08 (2H, d, J_{H-H} 6.4 Hz), 0.99 (2H, d J_{H-H} 6.4 Hz), 0.91 (3H, s), 0.47 (6H, s), and 0.42 (6H, s). $^{31}P\{^1H\}$ (298 K, C_6D_6): 48.8 (s). $^{13}C\{^1H\}$ (298 K, C_6D_6): 38.8 (t, J_{C-P} 5.5 Hz), 38.4 (t, J_{C-P} 5.5 Hz), 31.30 (s), 30.53 (s), 21.6 (t, J_{C-P} 10 Hz), 14.7 (br, s), 7.0 (s), 6.6 (s), −3.2 (t, J_{P-C} 8.6 Hz). IR (ν NO cm^{-1}, pentane): 1715

PNPRu(Me)(NO)Cl, 4. The crude $PNPRuMe_2$−PNPRu(Me)Cl mixture (0.030 g) was dissolved in 0.45 mL of C_6D_6 in a Youngs NMR tube. The solution was degassed three times and placed under 1 atm of NO gas, resulting in a color change on thawing to pale yellow. This yielded, by NMR spectroscopy, two products, **3** and **4**, in an approximate 4:1 ratio. Removal of benzene in vacuo, redissolving in minimum pentane, and storing at −40 °C overnight yielded a small number of X-ray quality crystals that a structure determination study proved to be PNPRu(Me)(NO)Cl. ^1H (298 K, C_6D_6): 1.73 (3H, t, J_{H-P} 9.6 Hz), 1.34 (36H, pseudoquartet, J_{H-P} 6 Hz), 1.18 (2H, d of t, J_{H-H} 11 Hz, J_{H-P} 4 Hz), 0.80 (2H, d of t, J_{H-H} 11 Hz, J_{H-P} 4.5 Hz), 0.38 (6H, s), and 0.32 (6H, s). $^1H\{^{31}P\}$ (298 K, C_6D_6): 1.73 (3H, s), 1.35 (18H, s), 1.33 (18H, s), 1.17 (2H, d, J_{H-H} 11 Hz), 0.80, (2H, d, J_{H-H} 11 Hz), 0.38 (6H, s) and 0.32 (6H, s). $^{31}P\{^1H\}$ (298 K, C_6D_6): 50.9 (s). IR (ν NO cm^{-1}, pentane): 1747.

PNPRu(H)$_3$, 5. A Youngs NMR tube was charged with $PNPRuMe_2$ (0.020 g, 0.035 mmol) and dissolved in 0.45 mL of C_6D_6. The solution was then degassed three times and backfilled with 1 atm of H_2. On shaking, the vermillion color rapidly dispersed, resulting in a yellow solution. The yield was quantitative by NMR spectroscopy. On standing in solution rapid H/D exchange between the hydride resonance and C_6D_6 occured, fully consistent with that seen previously for $PNP^{Cy}Ru(H)_3$.[43] On use of D_2, a 1:1:1 triplet for CH_3D was observed at 0.14 ppm (J_{H-D} 2.7 Hz). ^1H (298 K, C_6D_6): 1.13 (36H, t, J_{H-P} 6 Hz), 0.81 (4H, t, J_{H-P} 4.8 Hz), 0.45 (12H, s) −15.10 (3H, t, J_{H-P} 14 Hz). $^{31}P\{^1H\}$ (298 K, C_6D_6): 84.8 (s).

PNPRu(COMe)CO 6. $PNPRuMe_2$ (0.050 g, 0.087 mmol) was loaded into a sealable tube with a Teflon valve and was dissolved in 5 mL of toluene. The vermillion solution was degassed three times and backfilled with 1 atm of CO. Thawing and stirring the solution rapidly changed the color to pale yellow. The yield was quantitative by NMR spectroscopy, though the isolated yield was significantly lower. Removal of toluene in vacuo, redissolving in minimum pentane, and storing at −40 °C for 3 days yielded yellow crystals (0.020 g, 0.032 mmol). Yield: 37%. ^1H (298 K, C_6D_6): 2.82 (3H, s), 1.22 (18H, t, J_{H-P} 6.8 Hz), 1.19 (2H, partially overlapped signal), 1.12 (18H, t, 6.4 Hz), 1.05 (2H, t, 4 Hz), 0.50 (6H, s) and 0.37 (6H, s). $^1H\{^{31}P\}$ (298 K, C_6D_6): 2.82 (3H, s), 1.22 (18H, s), 1.19 (2H, br s), 1.12 (18H, s) 1.06 (2H, br s), 0.50 (6H, s), and 0.37 (6H, s). $^{31}P\{^1H\}$ (298 K, C_6D_6): 68.7 (s). IR (ν CO cm^{-1}, pentane): 1920, 1633. Mass spectrum (ESI+): calcd for (M + 1) $C_{25}H_{56}P_2Si_2O_2N_1Ru_1$, 622.3; exptl (M + 1), 622.4

Acknowledgment. This work was supported by the National Science Foundation. David Dye is thanked for his assistance in the EPR spectroscopy.

Supporting Information Available: Crystallographic details (.cif) for **1**, **2**, **4**, and **6** along with diagrams and data tables for **6**, the EPR spectrum of **2** (.pdf), and computational details for **1**. This material is available free of charge via the Internet at https://pubs.acs.org.

OM0508536